doi.org/10.15392/2319-0612.2026.2995
Braz. J. Radiat. Sci., Rio de Janeiro
Jul-Sep 2026, 14(3) | 01-19 | e2995
Editor(s): Dr. (Prof.) Bernardo Maranhão Dantas
Dr. (Prof.) Alfredo L. Ferreira Filho
Submitted: 2025-08-12
Accepted: 2026-04-15

Original Article

Response of a Commercial MOSFET to Clinical Photon and Electron Beams Used in Radiotherapy

Telles[a,b], L. F. K.; Maria[b], L. M.; Souza[c], D. N.; Santos[a], L. A. P.; Benevides[a], C. A.

[a]Comissão Nacional de Energia Nuclear (CNEN/CRCN-NE), 50.711-000, Recife, SE, Brazil
[b]Hospital Chama, 57.515-745, Arapiraca, AL, Brazil
[c]Departamento de Física, Universidade Federal de Sergipe, 49.107-230, São Cristóvão, SE, Brazil

*Correspondence: divanizia@gmail.com

Abstract: One type of dosimeter used in radiotherapy is the metal-oxide-semiconductor field-effect transistor (MOSFET), which is widely employed in *in vivo* dosimetry. This study investigated the response of a commercial MOSFET (STQ2HNK60ZR-AP) to photon and electron beams from a clinical linear accelerator. Radiation damage is typically associated with the dose received by the device and is reflected in shifts in the transistor's characteristic curve. In this work, however, a different approach was taken: the evaluated response was the beam-on drain current (I_D), integrated during beam exposure. The I_D under irradiation (I_{DX}) was obtained by subtracting the I_D measured without radiation, making the MOSFET functionally similar to an ionization chamber or diode detector. The transistor was placed between solid water plates in a 10 × 10 cm^2 radiation field, with a source-to-surface distance of 100 cm. I_{DX} was found to be directly proportional to the beam dose rate, and the collected charge showed minimal dependence on the dose rate (<3%). A Farmer ionization chamber was used as the reference detector. The MOSFET's response was linear with dose, and the energy dependence for photon beams was approximately 7% between 15 MV and 6 MV. The calibration factor varied by around 6% across different energies and beam types. These results highlight the need for correction factors when using a beam other than the calibration beam to meet the uncertainty threshold recommended by the International Commission on Radiation Units and Measurements for radiotherapy (±5%). The findings are consistent with previously published results and support the suitability of the MOSFET for dosimetry of photon beams from clinical linear accelerators. Future work will focus on evaluating clinical dosimetry parameters, including percentage depth dose, output factor, and beam profile.

Keywords: dosimetry, beam-on drain current, calibration beam, linear accelerator.

doi.org/10.15392/2319-0612.2026.2995
Braz. J. Radiat. Sci., Rio de Janeiro
Jul-Sep 2026, 14(3) | 01-19 | e2995
Editor(s): Dr. (Prof.) Bernardo Maranhão Dantas
Dr. (Prof.) Alfredo L. Ferreira Filho
Submitted: 2025-08-12
Accepted: 2026-04-15

Resposta de um MOSFET comercial a feixes clínicos de fótons e elétrons usados em radioterapias

Resumo: Um dos dosímetros usados em radioterapia é o transistor de efeito de campo de metal-óxido-semicondutor (MOSFET), amplamente empregado em dosimetria *in vivo*. Este estudo investigou a resposta de um MOSFET comercial (STQ2HNK60ZR-AP) a feixes de fótons e elétrons de um acelerador linear clínico. O dano por radiação é tipicamente associado à dose recebida pelo dispositivo e se reflete em deslocamentos na curva característica do transistor. Neste trabalho, no entanto, uma abordagem diferente foi adotada: a resposta avaliada foi a corrente de dreno (ID) do feixe, integrada durante a exposição ao feixe. A ID sob irradiação (I_{DX}) foi obtida subtraindo-se a ID medida sem radiação, tornando o MOSFET funcionalmente semelhante a uma câmara de ionização ou detector de diodo. O transistor foi posicionado entre placas de água sólida em um campo de radiação de 10 × 10 cm², com uma distância fonte-superfície de 100 cm. A I_{DX} medida foi diretamente proporcional à taxa de dose do feixe, e a carga coletada mostrou dependência mínima na taxa de dose (<3%). Uma câmara de ionização Farmer foi usada como detector de referência. A resposta do MOSFET foi linear com a dose, e a dependência energética em feixes de fótons foi de aproximadamente 7% entre 15 MV e 6 MV. O fator de calibração variou em cerca de 6% em diferentes energias e tipos de feixe. Esses resultados destacam a necessidade de fatores de correção ao se usar um feixe diferente do feixe de calibração, a fim de atender ao limite de incerteza recomendado pela Comissão Internacional de Unidades e Medidas de Radiação para radioterapia (±5%). Os resultados são consistentes com os publicados anteriormente e apoiam a adequação do MOSFET para dosimetria de feixes de fótons de aceleradores lineares clínicos. Trabalhos futuros se concentrarão na avaliação de parâmetros de dosimetria clínica, como porcentagem de dose em profundidade, fator de saída e perfil do feixe.

Palavras-chave: dosimetria, corrente de dreno, calibração de feixes, aceleradores lineares.

1. INTRODUCTION

Since the introduction of commercial linear accelerators in clinical practice, various dosimetry protocols for photon and electron radiotherapy beams have been published [1–4]. The literature describes several types of detectors, each with its own advantages and limitations depending on the specific dosimetric application. Among these, the ionization chamber (IC) is one of the most used detectors for calibrating clinical photon and electron beams in radiotherapy. Other radiation detectors used for this purpose include thermoluminescent detectors, films, diodes, and diamond detectors. Except for dosimetric films, all of these are solid-state detectors [1–4]. Solid-state detectors offer several advantages over other types, including their compact size (an essential feature for small-field dosimetry), good mechanical durability, and a stronger electrical response to radiation than other detectors [5–25].

Solid-state detectors include metal-oxide-semiconductor field-effect transistors (MOSFETs). Figure 1 illustrates a MOSFET, which consists of a silicon single crystal lightly doped to become p-type. Two islands of heavily doped n-type material are formed on the silicon substrate. The source and drain terminals are connected by a thin layer of n-type material that forms a channel. A thin layer of SiO_2 insulation is deposited over the device, and a metal layer is added on top to serve as the gate. Metal contacts are also placed over the drain and source, although they are electrically isolated from each other. If a drain-to-source voltage (V_{DS}) is applied, no current flows through the substrate because of the depletion barrier formed by the pn junction. However, when a positive gate-to-source voltage (V_{GS}) is applied, positive charges accumulate on the metal gate and induce negative charges in the channel by filling charge vacancies in the p-type substrate. This expands the channel between the islands. At a certain V_{GS}, known as the threshold voltage (V_{TH}), the channel becomes conductive. Figure 1 shows the formation of this electric field and illustrates why the device is referred to as a field-effect transistor.

During irradiation of a MOSFET, pairs of electrons and vacancies are generated throughout the oxide layer due to the breaking of Si–O_2 bonds. Some electrons recombine with the vacancies, while others are drawn toward the positive terminal of the V_{GS}. The remaining vacancies become trapped in the dielectric. These trapped vacancies generate an electric field that adds to the field from the applied VGS, widening the channel and lowering its resistivity. Radiation also induces changes in the charge carrier traps at the Si–SiO_2 interface. Together, these effects produce a drain current that is proportional to the dose rate, even when V_{GS} is below the V_{TH}. After irradiation, positive charge carriers remain in the insulator, and acceptor or donor traps at the interface continue to shift V_{TH}. This shift is proportional to the accumulated dose in the detector [25, 26].

Figure 1: MOSFET

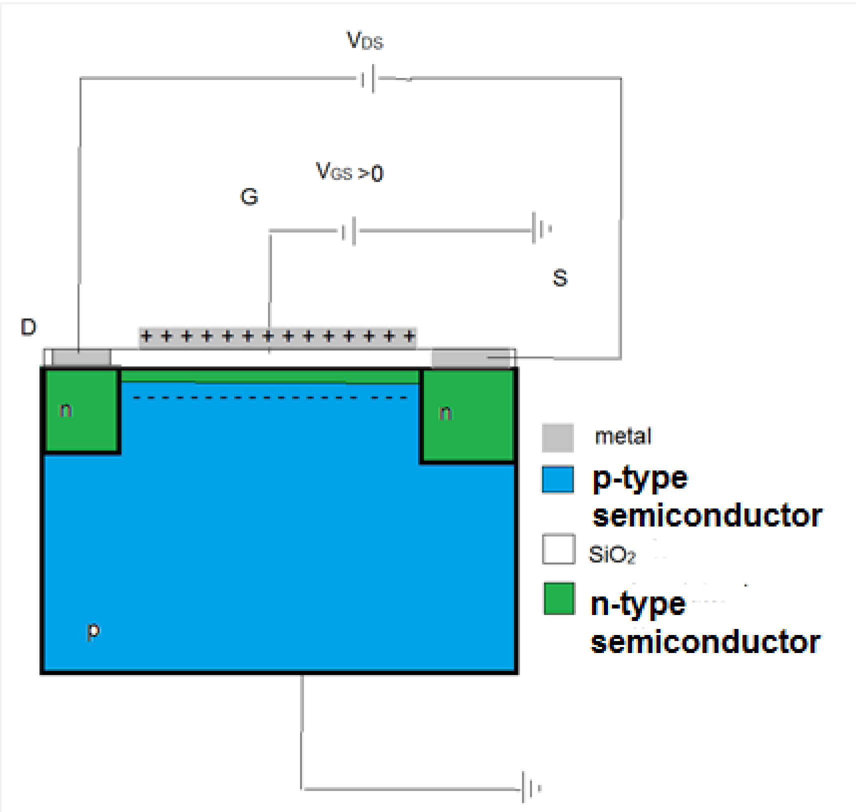

The working principle of a MOSFET as a detector is based on changes in its electrical response following irradiation. These changes result from damage caused by ionizing radiation interacting with the device's dielectric layer. This damage leads to a shift in the V_{TH}, and the variation (ΔV_{TH}) is directly proportional to the radiation dose recorded by the device within a specific dose range [5, 6, 16, 17, 19].

MOSFETs are widely used for real-time dosimetry [17, 19, 24, 25]. Kumar et al. [17] investigated the response of the TN502RD mobile MOSFET transistor (Best Medical Canada) as a function of dose, energy, dose rate, and photon beam angulation from 6 and 15 MV linear accelerators, as well as from a ^{60}Co source. The TN502RD contains a 1 mm^2 silicon chip with an active area of 0.2 × 0.2 mm^2. During testing, the MOSFETs were placed on a 10 cm acrylic phantom to ensure adequate backscatter. The calibration factor (cGy/mV) was determined by taking the ratio of the MOSFET's response, to the dose at the depth of maximum dose for each beam. The study concluded that the device's response was linear with dose and showed no dependence on energy, angle, or dose rate across all beam types. In a recent study, Kharusi et al. [24] examined diode and MOSFET dosimeters by simulating *in vivo* dosimetric procedures using an Alderson RANDO phantom. They derived correction factors based on radiotherapy protocols recommended by the International Atomic Energy Agency for *in vivo* dosimetry [27] and assessed the suitability of both diodes and MOSFETs for this application. When using MOSFETs as dosimeters, it is essential to consider their limited lifespan because their properties degrade after a certain number of uses.

This study was performed to evaluate the response of a commercial MOSFET (STQ2HNK60ZR-AP) when used as a detector for LINAC photon and electron beams. The operating principle of ICs and diodes is based on the accumulation of charge during irradiation. This study adopted the same principle, measuring the drain current (I_{DX}) during radiation exposure as the device's response to dose, rather than tracking changes in V_{TH} with dose [17]. The evaluation focused on the dose response, dose rate dependence, energy dependence, and maximum accumulated dose beyond which the transistor loses its linear behavior.

The STQ2HNK60ZR-AP MOSFET is a 600 V, 3.5 Ω (typical), 500 mA n-channel SuperMESH power transistor. Several factors motivated the use of this device: its compact size (approximately 5 mm × 5 mm); its TO-92 chip design, which facilitates insertion into a PMMA phantom; its low operating voltage (5 V); its affordability; and the availability of three types of encapsulation, which will allow for comparative analysis in future studies. The device's structure includes a silicon chip of approximately 2 mm^2, which is assumed to represent the sensitive area in this work. Figure 2 shows the internal structure of the MOSFET as revealed by radiography.

Figure 2: MOSFET dimensions

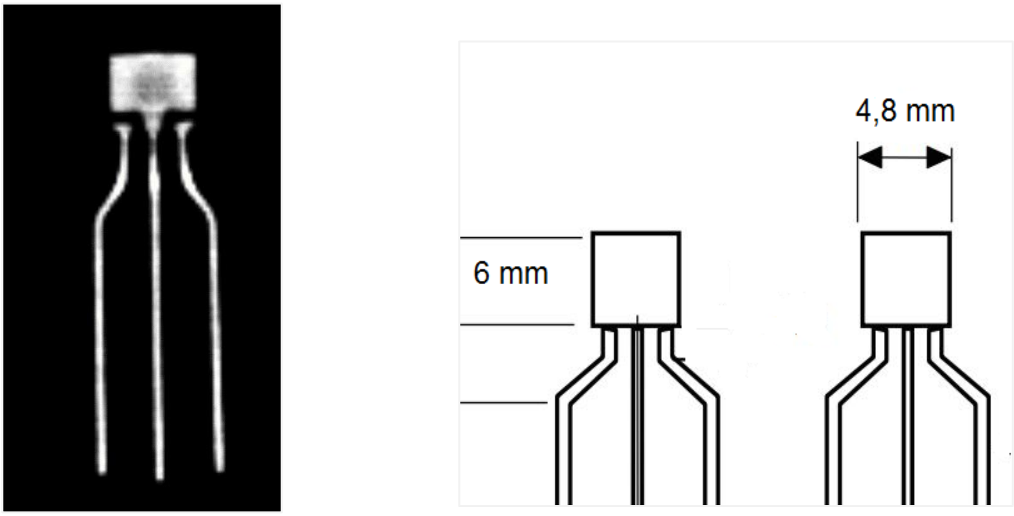

The transistor's electrical behavior can be divided into three regions based on V_{GS}: the cut-off region, the active region, and the saturation region. The cut-off region spans from 0.0 V to approximately 3.3 V (I_D < 5 nA); the active region extends from 3.4 to 3.9 V, where the curve exhibits high sensitivity; and the saturation region ranges from roughly 3.9 to 5.0 V, where $I_D = V_{DS}/R_D$. Based on V_{DS}, a 500 kΩ R_D resistor was selected, resulting in a saturation current of 10 µA.

2. MATERIALS AND METHODS

2.1 MOSFET Signal Measurement System

Initially, the electrical switching curves of 50 devices from the same manufacturing batch were recorded. Eight of these devices were selected for irradiation based on their matching I_D, which varied by less than ±1%. Due to the study's methodological rigor, a small sample size was sufficient to obtain the presented data [28].

Given the resolution of the EFF1705 measurement system from Scients®, which was used to supply V_{GS} and V_{DS} and to measure I_D simultaneously, the measurement uncertainty for I_D at each point on the curve is 0.1 nA. The initial I_D of a MOSFET can vary before irradiation, depending on the specific MOSFET type. Additionally, I_D may vary across devices within the same manufacturing batch, despite the fabrication process being fully automated and highly precise.

During irradiation of a MOSFET, the I_D increases due to interactions between the radiation beam and both the chip and its encapsulation. For this reason, it is helpful to distinguish the I_D under irradiation (I_{DX}) from the baseline I_D [16]. I_{DX} refers to the current measured during irradiation, excluding the parasitic current generated by the electric field resulting from ionization-induced damage to the MOSFET's dielectric. In this study, I_D was less than 5 nA before irradiation and varied depending on the dose to which the devices were exposed.

2.2 Clinical Linear Accelerator and Radiation Beams

All experiments were conducted using a Varian IX linear accelerator. Measurements were taken with a MOSFET inserted into a 3 mm-thick PMMA plate (density: 1.18 g/cm^3) sandwiched between layers of solid water. The solid water layer beneath the device was 5 cm thick. For photon beam irradiations (6 and 15 MV), an additional 5 cm layer of solid water was placed above the MOSFET. For electron beam irradiations at 6, 9, 12, 16, and 20 MeV, the devices were positioned at depths of 1, 2, 3, 4, and 2 cm, respectively. A standard field size of 10 × 10 cm² was used for all irradiations, and the source-to-surface distance was set to 100 cm.

According to TRS 483, the dose conversion factor for the solid water phantom relative to water differs by less than 1% for the photon energies used in this study. Therefore, for this work, the conversion factor was taken as 1 for both photon and electron beams.

2.3 Irradiation Procedures

In this study, the response of the irradiated detector was defined as the integration of I_{DX} during beam-on time, measured as charge in nanocoulombs (nC). Six irradiation procedures were conducted to evaluate the MOSFET response: (a) analysis of the I_{DX} signal as a function of the dose rate, (b) response of the detector to the dose, (c) response as a function of the irradiation beam energy, (d) response in relation to V_{GS} variation, (e) the calibration factor with respect to the dose rate, and (f) response to the accumulated dose. For photon beam irradiation, the accelerator was equipped with a flattening filter. The reference detector used for absolute dose measurements was a 0.6 cc Farmer IC (PTW®), calibrated in a secondary standards laboratory. Electron beam calibration was performed using a TN34001 parallel-plate IC (PTW®), which was cross-compared with the Farmer IC. Table 1 presents the MOSFET labels along with their corresponding irradiation beam types.

Table 1: Coefficient of determination (R^2) for the linear fit of the dose–response curve for each MOSFET and beam type

BEAM		MOSFETs	ACCUMULATED DOSE (cGy)	R^2 (linear fit)
TYPE	ENERGY			
Electron	6 MeV	1	2610	0.9984
	9 MeV	1, 2	4892, 1000	0.9930
	12 MeV	2	3610	0.9981
	16 MeV	2, 6	6920, 5290	0.9295, 0.9991
	20 MeV	3	2610	0.9998
Photon	6 MV	4	4290	0.9999
	15 MV	5	4290	0.99998

Note: V_{GS} = 2.7 V

3. RESULTS AND DISCUSSIONS

Figure 3 shows how I_{DX} varied with dose rate for both photon and electron beams. The graph demonstrates the linearity of the I_{DX} signal with respect to dose rate for each irradiation beam type. Table 2 presents the average charge measured during the calibration of the MOSFETs irradiated with a 100 cGy dose from five different beams (two photon and three electron). The dose rates ranged from 100 to 600 monitor units per minute (MU/min) for photon beams and from 100 to 1000 MU/min for electron beams. The standard deviation reflects the variation in response to different dose rates.

Figure 3: Drain current under irradiation (I_{DX}) as a function of dose rate for photon and electron beams

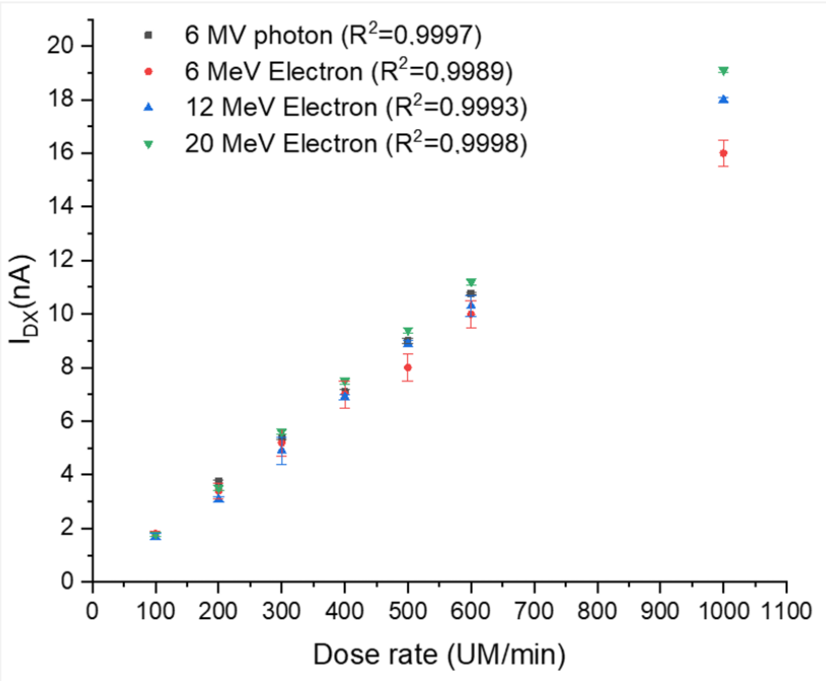

Table 2: Average charge measured for a 100 cGy dose at various dose rates (100–1000 MU/min)

ENERGY	AVERAGE CHARGE (nC)	STANDARD DEVIATION (%)	V_{GS} (V)	CALIBRATION FACTOR (cGy/nC)
6 MeV	110.20	1.50	2.70	0.91
12 Mev	104.00	2.50	2.70	0.96
20 MeV	111.00	2.50	2.70	0.91
15 MV	107.35	2.00	0.50	0.93
6 MV	110.60	2.50	0.50	0.90

Note: Measurements were taken at the indicated V_{GS} for each beam.

Due to their low mass, electrons undergo significant deflection when interacting with the electric fields of nuclei. Therefore, angular scattering is more pronounced at lower energies, such as 6 MeV, than at higher energies (e.g., 15 MeV), which impsct in stopping power rations. This results in greater lateral scattering and rapid broadening of the beam penumbra as it penetrates material [29]. However, this aspect was not considered in this study because the placement depth and centrality of the MOSFETs in the radiation field were not thought to affect the doses to which the devices were exposed.

Before analyzing the MOSFET's dose response, an irradiation experiment was performed to determine the maximum suitable V_{GS}, as V_{TH} decreased with accumulated dose. This step helped avoid using a V_{GS} value that fell within the active region of the MOSFET's switching curve. The results are shown in Figure 4. As illustrated, biasing the MOSFET with V_{GS} = 0.5 V was sufficient provided the accumulated dose did not exceed 50,000 cGy. Figure 5 shows the dose–response curves for the six device samples over the range of 0-10,000 cGy, as described in Table 1. The table also presents the correlation coefficients (R^2) of the linear fits. Both figures demonstrate strong linearity, with each device exhibiting its own sensitivity, as it is characteristic of all detector types.

Figure 4: Switching curve: MOSFET 2

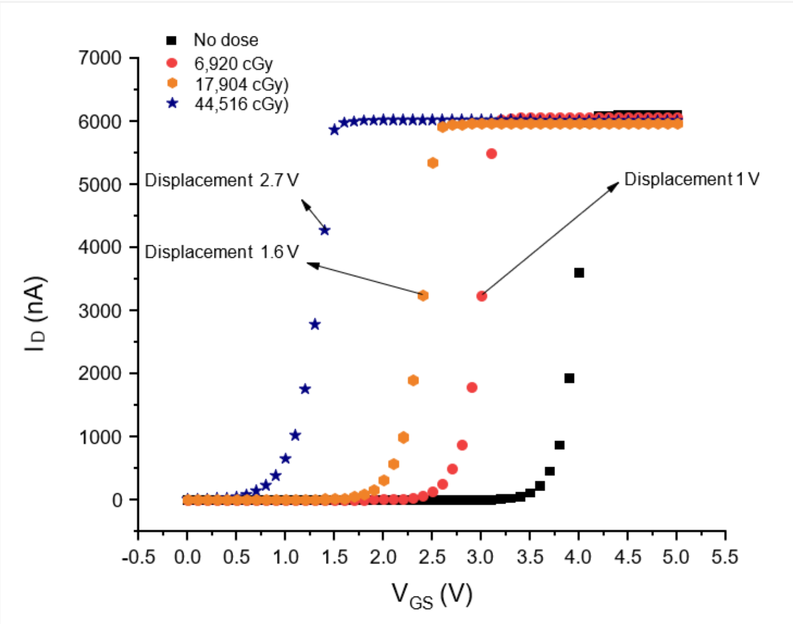

Figure 5: Dose–response curve (V_{GS} = 2,7 V)

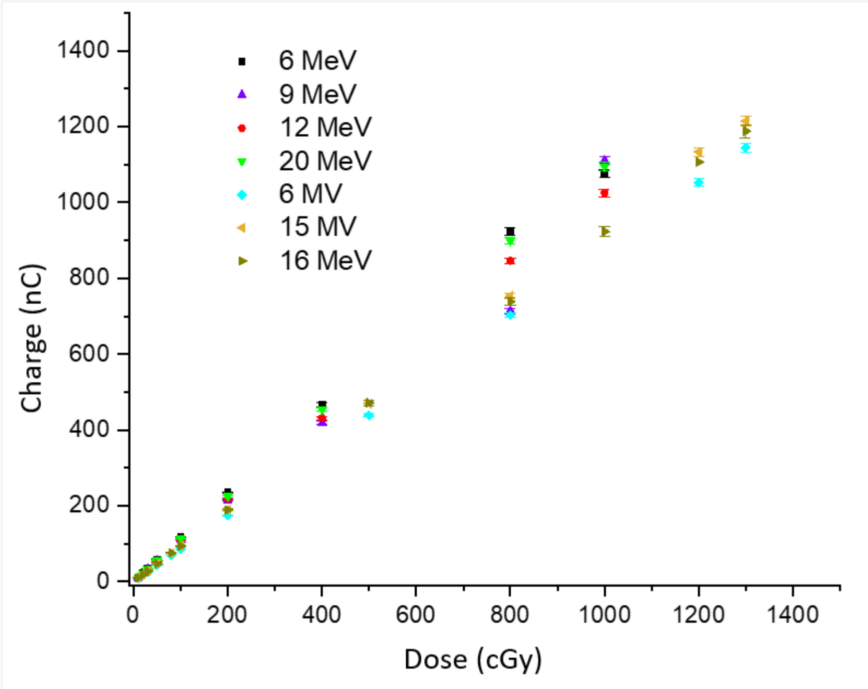

Figure 6 illustrates the MOSFET's behavior under varying radiation beam energies. A 7% difference was observed in the slope of the 15 MV photon beam response compared with that of the 6 MV photon beam.

Figure 6: Charge measured as a function of dose (dose response)

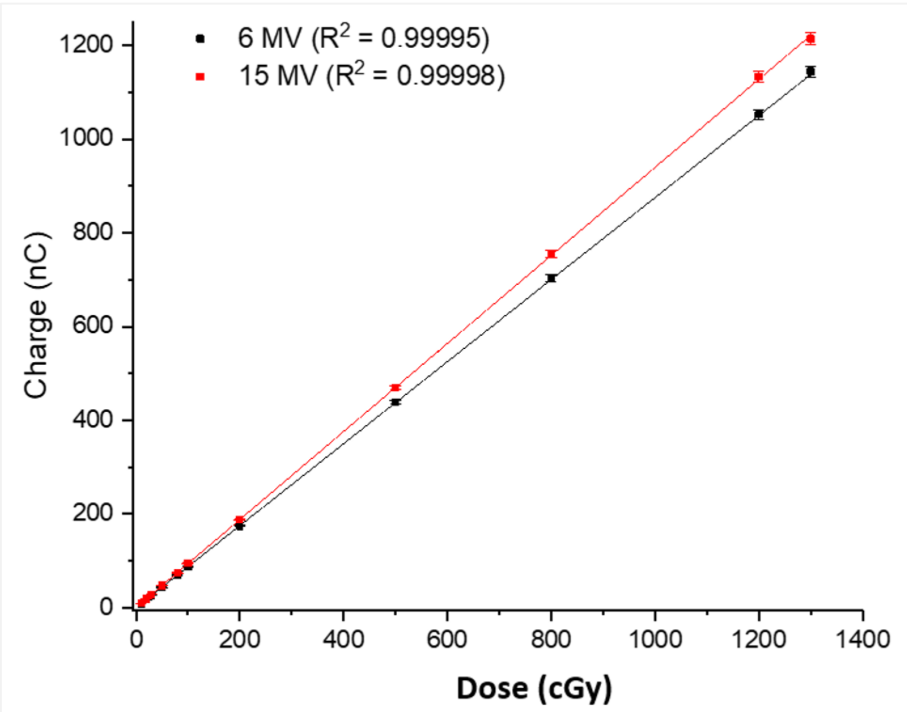

Finally, the V_{GS} was varied using the same device, adjusting it by the same amount that the switching curve shifted due to the accumulated dose (see Figure 4). Figure 7 shows that this change had no effect on the linearity of the device's response, provided that its value is not in the switching curve. Figure 5 presents the result obtained with V_{GS} = 2.7 V.

Figure 7: Response of the MOSFET as a function of dose following V_{GS} change

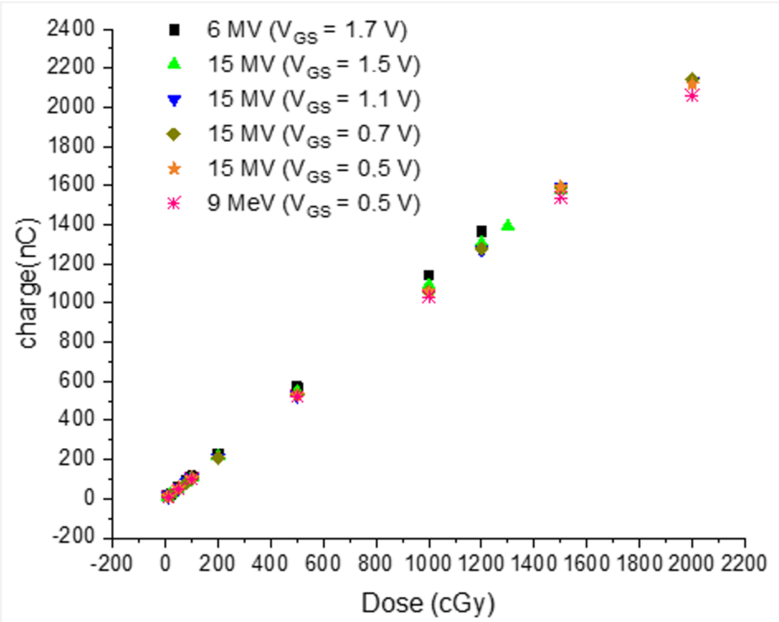

The results of this study are consistent with those reported by Kumar et al. [17] and Manigandan et al. [6] regarding the linearity of the MOSFET's response. However, Manigandan et al. [6] noted the need for a correction factor to address nonlinearity in responses below 20 cGy, which was a behavior not observed in the present study. Kumar et al. [17] found that the MOSFET dosimeter's response was low dependent of photon energy, with a maximum variation of approximately ±1%. By contrast, this study revealed 7% variation across the photon energy range used and 6% across all beams (see Figure 6 and Table 2). This dependence may be due to variation in the attenuation of the beams caused by encapsulating the MOSFET. Further studies should investigate the factors influencing this energy dependence. Additionally, the MOSFET response showed low dependence from variations, with deviations of less than 3%, which is a result that aligns with the specifications provided by the LINAC manufacturer (VARIAN), which states a dose rate-related variation of ±1% in its acceptance documentation [29]. This means that the generated signal is directly proportional to the number of radiation interactions per unit time. Therefore, there was no signal saturation or differentiated recombination effects as a function of dose rates within the studied interval. Throughout this study, V_{DS} was held constant at 5 V. An average shift of −0.01 V/Gy in the switching curve was observed with increasing accumulated dose. When V_{GS} was adjusted by the same amount, the device's response remained linear. As already mentioned, this statement is only true when this value is not found on the switching curve. This supports findings by Kumar et al. [17], who demonstrated that the transistor's response does not depend on gate voltage if it remains below the V_{TH}, which was also confirmed in our experiments. Schwank et al. [26] report that high concentrations of interface-trap charge can reduce carrier mobility and increase the V_{TH} in n-channel MOS transistors. However, in this study, the opposite effect was observed. This aligns with another conclusion by Schwank et al. [26], who noted that a positive charge associated with trapped holes causes a negative shift in V_{TH} in both n and p-channel MOS transistors. Data in Table 1 further confirm that radiation damage was not uniform across all MOSFETs, even within the same manufacturing batch. As shown in Table 2, the largest variation in the calibration factor was approximately 6% for both photon and electron beams. For comparison, Kumar et al. [17] reported up to a 20% difference in this factor when comparing a 15 MV beam to a 6 MV beam [17]. According to the International Commission on Radiation Units and Measurements [30], the dose delivered to a patient must be known with a maximum uncertainty of ±5%. Therefore, if the device is calibrated at a specific photon or electron energy, this study shows that correction factors are necessary for its use in beams of different energies, similar to the approach used for ionization chambers in TRS 398 [31].

4. CONCLUSIONS

The STQ2HNK60ZR-AP MOSFET proved to be a viable radiation detector for clinical beams. This study demonstrated that, by using charge measurement, results comparable in linearity and dose-rate dependence to those obtained in [17]. The operational range of the device was found to be up to 50,000 cGy when biased at V_{GS} = 0.5 V. Because radiation damage in this work resulted in a decrease in V_{TH}, it can be inferred that oxide vacancy traps were the dominant mechanism of radiation-induced damage.

Relative measurements, such as percentage depth dose, output factor, and beam profile, may be the most suitable applications for this transistor because such measurements are ideal for detectors with low energy dependence. Consequently, future work will focus on evaluating clinical dosimetry parameters, which may establish this device as a candidate for applications beyond *in vivo* dosimetry.

ACKNOWLEDGMENT

The authors thank the Brazilian agencies Comissão Nacional de Energia Nuclear (CNEN), Brazilian Innovation Agency (FINEP), Coordenação de Aperfeiçoamento de Pessoal de Nível Superior (CAPES) and Conselho Nacional de Desenvolvimento Científico e Tecnológico (CNPq - National Institute of Radiation Technology in Health Science, INTERAS - 406761/2022–1).

FUNDING

Brazilian agency Comissão Nacional de Energia Nuclear (CNEN).

CONTRIBUTORSHIP

Conceptualization: TLFK, MLM, SDN, SLAP, BCA

Investigation: TLFK, MLM, SDN, SLAP, BCA

Writing – review and editing: TLFK, MLM, SDN, SLAP, BCA

CONFLICT OF INTEREST

All authors declare that they have no conflicts of interest.

DATA AVAILABILITY STATEMENT

Interview transcripts and qualitative data are not publicly available due to confidentiality commitments made to research participants. Aggregated data supporting the findings are available from the corresponding author upon reasonable request and subject to participant privacy protections.

REFERENCES

[1] KHAN, F. M. Clinical electron-beam dosimetry: report of AAPM Radiation Therapy Committee Task Group 25. **Medical Physics**, v. 18, p. 73-109, 1991.

[2] ICRU - INTERNATIONAL COMMISSION ON RADIATION UNITS AND MEASUREMENTS. **Radiation Dosimetry**: electrons with initial energies between 1 and 50 MeV. Bathesda: ICRU, 1972. (ICRU Report 21).

[3] ICRU - INTERNATIONAL COMMISSION ON RADIATION UNITS AND MEASUREMENTS. **Dose Specification for Reporting External Beam Therapy with Photons and Electrons**. Bathesda: ICRU, 1978. (ICRU Report 29).

[4] ICRU - INTERNATIONAL COMMISSION ON RADIATION UNITS AND MEASUREMENTS. **Radiation Dosimetry**: electron beams with energies between 1 and 50 MeV. Bathesda: ICRU, 1984. (ICRU Report 35).

[5] SANTOS, L. A. P. An overview on bipolar junction transistor as a sensor for x-ray beams used in medical diagnosis. **Sensors**, v. 22, p. 1-18, 2022. Disponível em: https://doi.org/10.3390/s22051923.

[6] MANIGANDAN, D. et al. Dosimetric characteristics of a MOSFET dosimeter for clinical electron beams. **Physica Medica**, v. 25, p. 141-147, 2009. Disponível em: https://doi.org/10.1016/j.ejmp.2008.11.003.

[7] IAEA – INTERNATIONAL ATOMIC ENERGY AGENCY. **TRS 483**: dosimetry of small static fields used in external beam radiotherapy. Vienna: IAEA, 2017.

[8] MCGRATH, A. N.; GOLMAKANI, S.; WILLIAMS, T. J. Determination of correction factors in small MLC-defined fields for the Razor and microSilicon diode detectors and evaluation of the suitability of the IAEA TRS-483 protocol for multiple detectors. **Journal of Applied Clinical Medical Physics**, v. 23, n. 7, p. e13657, 2022. Disponível em: https://doi.org/10.1002/acm2.13657.

[9] AKINO, Y. et al. Characterization of a new commercial single crystal diamond detector for photon-and proton-beam dosimetry. **Journal of Radiation Research**, v. 56, n. 6, p. 912-918, 2015. Disponível em: https://doi.org/10.1093/jrr/rrv044.

[10] CARRASCO, P. et al. Characterization of the Exradin W1 scintillator for use in radiotherapy. **Medical Physics**, v. 42, p. 297–304, 2015. Disponível em: https://doi.org/10.1118/1.4903757.

[11] PAPACONSTADOPOULOS, P.; TESSIER, F.; SEUNTJENS, J. On the correction, perturbation and modification of small field detectors in relative dosimetry. **Physics in Medicine & Biology**, v. 59, n. 19, p. 5937, 2014. Disponível em: https://doi.org/10.1088/0031-9155/59/19/5937.

[12] AKINO, Y. et al. Characterization of a microSilicon diode detector for small-field photon beam dosimetry. **Journal of Radiation Research**, v. 61, n. 3, p. 410–418, 2020. Disponível em: doi.org.

[13] CASAR, B. et al. A novel method for the determination of field output factors and output correction factors for small stactic fields for six diodes and a microdiamond detector in megavoltage photon beams. **Medical Physics**, v. 46, n. 2, p. 944-963, 2019. Disponível em: https://doi.org/10.1002/mp.13318.

[14] AKINO, Y. et al. Characteristics of microSilicon diode detector for electron beam dosimetry. **Journal of Radiation Research**, v. 62, n. 6, p. 1130–1138, 2021. Disponível em: https://doi.org/10.1093/jrr/rrab085.

[15] HAIJUN, C. et al. Limitations of Silicon Diodes for clinical electron Dosimetry. **Radiation Protection Dosimetry**, v. 120, p. 56-59, 2006. Disponível em: doi.org.

[16] CAVALCANTI, F. A.; SANTOS, L. A. A MOSFET-based method for measuring peak kilovoltage (kVp) in Diagnostic X-Ray Beams. **IEEE Open Journal of Instrumentation and Measurement**, v. 1, p. 1-7, 2022. Disponível em: https://doi.org/10.1109/OJIM.2022.3196725.

[17] KUMAR, A. S.; SHARMA, S. D.; RAVINDRAN, B. P. Characteristics of mobile MOSFET dosimetry system for megavoltage photon beams. **Journal of Medical Physics**, v. 39, n. 3, p. 142-149, 2014. Disponível em: https://doi.org/10.4103/0971-6203.139002.

[18] KALEF EZRA, J. A. et al. Thermoluminescence dosimetry for quality assurance in radiation therapy. **Radiation Protection Dosimetry**, v. 101, p. 403-405, 2002. Disponível em: https://doi.org/10.1093/oxfordjournals.rpd.a006011.

[19] SOUBRA, M.; CYGLER, J.; MACKAY, G. Evaluation of a dual bias dual metal oxide silicon semiconductor field effect transistor detector as radiation dosimeter. **Medical Physics**, v. 21, p. 567-572, 1994. Disponível em: https://doi.org/10.1118/1.597314.

[20] AL MOHAMMED, H. I. Evaluation of clinical use of OneDose metal oxide semiconductor field effect transistor detectors compared to thermoluminescent dosimeters to measure skin dose for adult patients with acute lymphoblastic leukemia. **North American Journal of Medical Sciences**, v. 3, n. 8, p. 362, 2011. Disponível em: https://doi.org/10.4297/najms.2011.3362.

[21] XIANG, H. F. et al. Build up and surface dose measurements on phantoms using micro MOSFET in 6 and 10 MV x ray beams and comparisons with Monte Carlo calculations. **Medical Physics**, v. 34, n. 4, p. 1266-1273, 2007. Disponível em: https://doi.org/10.1118/1.2710951.

[22] GONÇALVES FILHO, L. C. et al. Radiation dose response of n-channel MOSFET submitted to filtered X-ray photon beam. **IEEE Transactions on Nuclear Science**, v. 65, n. 9, p. 2607-2610, 2018. Disponível em: https://doi.org/10.1109/TNS.2018.2846668.

[23] CHEN, A. X. et al. Compact Ion Beam System for Fusion Demonstration. **Physics Open**, v. 21, p. 100234, 2024. Disponível em: https://doi.org/10.1016/j.physo.2024.100234.

[24] AL KHARUSI, O. et al. Commissioning and performance assessment of diodes and MOSFETs in in-vivo dosimetry for external beam radiation therapy. **Radiation and Environmental Biophysics**, p. 1-15, 2025. Disponível em: https://doi.org/10.1007/s00411-025-01117-3.

[25] SIEBEL, O. F. **Desenvolvimento de um dosímetro in vivo a MOSFET para aplicações em radioterapia**. 2013. Tese (Doutorado em Engenharia Elétrica) – Universidade Federal de Santa Catarina, Florianópolis, 2013. Disponível em: https://repositorio.ufsc.br/handle/123456789/122778. Acesso em: 10 ago. 2025.

[26] SCHWANK, J. R. et al. Radiation effects in MOS oxides. **IEEE Transactions on Nuclear Science**, v. 55, n. 4, p. 1833-1853, 2008. Disponível em: https://doi.org/10.1109/TNS.2008.2001040.

[27] INTERNATIONAL ATOMIC ENERGY AGENCY. **IAEA Health Report No. 8**: development of procedure for in vivo dosimetry in radiotherapy. Vienna: IAEA, 2013.

[28] BEKMEZCI, Mustafa et al. Determining Validity, Reliability, and Sample Size in Qualitative Research. **PaperASIA**, v. 41, n. 4b, p. 287-300, 2025.

[29] ANDREO, P. et al. Influence of energy and angular spread on stopping-power ratios for electron beams. **Physics in Medicine & Biology**, v. 34, n. 6, p. 751-768, 1989.

[30] ICRU - INTERNATIONAL COMMISSION ON RADIATION UNITS AND MEASUREMENTS. **Determination of absorbed dose in a patient irradiated by beams of X or gamma rays in radiotherapy procedures**. Washington: ICRU, 1976.

[31] ANDREO, P. et al. **Absorbed dose determination in external beam radiotherapy**: an international Code of Practice for dosimetry based on standards of absorbed dose to water. Vienna: International Atomic Energy Agency, 2000. (IAEA Technical Report Series, n. 398).

LICENSE